Dispersal and fire limit Arctic shrub expansion

Yanlan Liu (liu.9367@osu.edu)
The Ohio State University https://orcid.org/0000-0001-5129-6284
William Riley
Lawrence Berkeley National Laboratory https://orcid.org/0000-0002-4615-2304
Trevor Keenan
UC Berkeley https://orcid.org/0000-0002-3347-0258
Zelalem Mekonnen
Lawrence Berkeley National Laboratory https://orcid.org/0000-0002-2647-0671
Jennifer Holm
Lawrence Berkeley National Laboratory
Qing Zhu
Lawrence Berkeley National Laboratory https://orcid.org/0000-0003-2441-944X
Margaret Torn
Lawrence Berkeley National Laboratory https://orcid.org/0000-0002-8174-0099

Article

Keywords:

Posted Date: December 2nd, 2021

DOI: https://doi.org/10.21203/rs.3.rs-1048197/v1

Version of Record: A version of this preprint was published at Nature Communications on July 4th, 2022.
See the published version at https://doi.org/10.1038/s41467-022-31597-6.

Dispersal and fire limit Arctic shrub expansion

Yanlan Liu[1,2,3]*, William J. Riley[3], Trevor F. Keenan[3,4], Zelalem A. Mekonnen[3], Jennifer A. Holm[3], Qing Zhu[3], Margaret S. Torn[3]

[1]School of Earth Sciences, The Ohio State University, Columbus, OH, USA

[2]School of Environment and Natural Resources, The Ohio State University, Columbus, OH, USA

[3]Climate and Ecosystem Sciences Division, Lawrence Berkeley National Laboratory, Berkeley, CA, USA

[4]Department of Environmental Science Policy and Management, University of California, Berkeley, CA, USA

*Email: liu.9367@osu.edu

Abstract

Arctic shrub expansion has been widely reported in recent decades, with large impacts on carbon budgets, albedo, and warming rates in high latitudes. However, predicting shrub expansion across regions remains challenging because the underlying controls remain unclear. Observational studies and models typically use relationships between observed shrub presence and current environmental suitability (climate and topography) to predict shrub expansion, but such approaches omit potentially important biotic-abiotic interactions and non-stationary relationships. Here, we use long-term high-resolution satellite imagery across Alaska and western Canada to show that observed shrub expansion has not been controlled by environmental suitability during 1984-2014, but rather can only be explained by accounting for seed dispersal and fire. These findings provide the impetus for better observations of recruitment and for incorporating currently underrepresented processes of seed dispersal and fire in land models to project shrub expansion and future climate feedbacks. Integrating these dynamic processes with projected fire extent and climate, we estimate that shrubs will expand into 25% of the non-shrub

tundra by 2100, in contrast to 39% predicted using a relationship with increasing suitability alone. Thus, using environmental suitability alone likely overestimates and misrepresents the spatial pattern of shrub expansion and its associated carbon sink.

Main

The Arctic has warmed more than twice as fast as the global average and is projected to continue outpacing lower latitudes over the 21st century[1]. Rapid climate warming in recent decades and associated feedbacks have led to shifts in Arctic vegetation composition and abundance[2–4]. In particular, increased tundra shrub cover has been widely observed through field surveys[5], aerial photographs[6,7], and satellite remote sensing[8,9]. Pervasive shrub expansion can heat the atmosphere through decreased albedo and increased greenhouse warming induced by atmospheric water vapor, resulting from increased evapotranspiration and regional ocean feedbacks[10–12]. Locally, shrubs can warm the soil in the winter due to insulation of accumulated snow, which deepens the active layer and accelerates soil carbon loss compared to non-shrub tundra[13,14]. Moreover, the distribution of shrubs also affects nutrient cycling, animal populations[15], and wildfire risk and associated carbon emissions[16,17]. Understanding controls of shrub expansion patterns is therefore crucial to predicting climate feedbacks and ecological consequences of the rapidly changing Arctic.

The area where temperature limits the growth of Arctic vegetation has been declining over the past decades[18]. Increasing temperature has been identified as a major control of shrub expansion[5,19,20]. However, the influence of temperature can be attenuated or reversed by soil moisture limitation, snow distribution, and topography[4,21–25]. The majority of observational-based studies focus on environmental factors and attribute the heterogeneity of shrub expansion

to spatial variation of environment-based suitability, i.e., the likelihood of shrub presence given environmental conditions[26]. Based on space-for-time substitutions, some of those studies used derived spatial environment-vegetation relationships to assess future shrub expansion[5,20,21], assuming stationary relationships between species and the environment. Although this approach has been found effective in predicting species distributions when ecosystems are in dynamic equilibrium, e.g., under a relatively stable climate or over a sufficiently long time scale[27], it ignores transient responses and non-stationary ecological processes, thus causing errors in projected ecosystem change[28–30]. As the Arctic tundra deviates from the historical quasi-equilibrium due to climate change, evaluating the dynamic roles of plant migration and disturbance becomes especially relevant.

With changes in growing conditions under a warmer climate, successful establishment of new shrub patches depends on seed dispersal. Seeds can be dispersed through many biotic and abiotic vectors, such as gravity, animals, wind, ocean currents, and drifting sea ice, which result in dispersal ranges from meters to hundreds of kilometers[31,32]. Seed dispersal has been found important in explaining shifts in vegetation composition at sites in alpine[33], mediterranean[34,35], and tropical biomes[36,37]. Nonetheless, the impact of seed dispersal on vegetation patterns is also compounded by suitable environmental niches and thus is not always the limiting factor [38–40]. In the Arctic, genetic analysis has revealed repeated long-distance seed dispersal to a remote archipelago from multiple source regions since the last glacial retreat, while the resulting species distribution is predominantly shaped by temperature that limits suitability for establishment[39]. In contrast to a relatively stable climate over the past several millennia, the fast changing climate over recent decades might lead to shifts in the relative dominance of environmental suitability and seed dispersal in shaping Arctic shrub expansion.

71 The dynamic trajectory of ecosystems may also be affected by disturbance. Although
72 historically rare in Arctic ecosystems, wildfire is expected to become more intense and frequent
73 as the climate warms[16,41]. In the short term, wildfires may cause seed and seedling mortality,
74 which could limit post-fire recruitment. On the other hand, wildfires can alter post-fire
75 vegetation trajectories by heating the soil during the fire, cause long-term soil warming by
76 removing surface litter, and improve seedbed nutrient availability, thus facilitating germination
77 and seedling establishment[42–46]. For example, modeling and site-based field studies have
78 reported both enhanced expansion and diminished recovery of shrubs from four years to two
79 decades after wildfires at several sites in Alaska[43,45,47–49]. How wildfires affect shrub expansion
80 across large gradients of environmental suitability and seed dispersal has barely been evaluated
81 using observations.
82 We focused on shrub expansion from 1984 to 2014 across the northwestern region of
83 North America covering Alaska and western Canada, i.e., the NASA Arctic-Boreal Vulnerability
84 Experiment (ABoVE) core domain. Shrub expansion was detected using an annual dominant
85 land-cover product derived from Landsat surface reflectance and trained over field photography
86 and very high resolution imagery[3]. Here, shrub expansion is defined as shrub dominance in
87 tundra originally dominated by non-woody species at a 30 m scale. We collected topographic
88 and regionally downscaled bioclimatic variables across the domain to identify the variables most
89 informative for observed shrub expansion (Methods). Based on these selected topographic and
90 bioclimatic conditions, averaged over three decades prior to 1984, we estimated environmental
91 suitability for shrubs in 1984 using a random forest model. The same model was then used to
92 calculate the suitability for shrubs in 2014 using 1985-2014 average bioclimatic conditions. We
93 analyzed whether changes in suitability could explain shrub expansion from 1984 to 2014. Seed

arrival probability, a measure of spatial proximity to existing shrub patches, was calculated through convolution of seed-dispersal kernels over 1984 shrub cover images. Given the variety of dispersal mechanisms, we considered both short- and long-distance dispersal kernels, and optimized the range and shape parameters to fit observed shrub expansion. The year and location of fires were obtained from a Landsat-derived annual burn scar product. We investigated individual and compound impacts of environmental suitability, seed dispersal, and fire occurrence on observed 1984-2014 shrub expansion. Based on the resulting sensitivities and the projection of bioclimatic conditions and fire from climate models, we estimated shrub expansion in 2040, 2070, and 2100, and explored the relative importance of suitability change, fire, and seed dispersal on projected shrub expansion.

Environmental suitability of shrubs

We first estimated bioclimatic and topographic suitability for shrubs as of 1984. Among the 27 variables, the seven most informative variables, as identified based on variance inflation factors (Extended Data Table 1, Extended Data Fig. 1), were three bioclimatic variables (degree days above 5 ℃, annual heat moisture index, and precipitation as snow) and four topographic variables (elevation, slope, aspect, and topographic wetness index). Based on the random forest model, degree days above 5 ℃ was the most important variable for suitability in 1984, followed by elevation and precipitation as snow (Fig. 1a). In terms of the direction and shape of response, higher suitability was associated with higher degree days above 5 ℃, lower elevation, and higher precipitation as snow (Extended Data Fig. 2), although suitability responds to these variables nonlinearly across different combinations of climate and topographic conditions (Extended Data Fig. 3).

Suitability conditions in 1984 were higher in southwestern Alaska, eastern Seward Peninsula, and northern Northwest Territories of Canada, but lower on the northern edge of the North Slope of Alaska and northern Canada and mountainous regions such as the Brooks Range and the Mackenzie Mountains (Fig. 1a, reference locations noted in Extended Data Fig. 1c). This pattern of suitability was largely consistent with observed shrub distribution in 1984 ($r = 0.92$, Fig. 1b), supporting the effectiveness of the suitability metric in describing the shrub-environment relationship under quasi-equilibrium conditions. Due to climate warming since 1984, the domain became more suitable in 2014 on average, especially in southwestern Alaska, eastern Seward Peninsula, the North Slope, and the southeast of the domain (Fig. 1c). The area with high suitability (> 0.4) increased from 13.4% to 28.3% of the region. However, these highly suitable regions experienced limited shrub expansion (Fig. 1d). Instead, hot spots of shrub expansion were found in the west of the North Slope and northwestern Canada. Across the entire domain, suitability was much less related to new (i.e., expanded) shrub area in 2014 ($r = 0.35$) than to existing shrub cover in 1984 ($r = 0.92$). Accounting for different initial land cover types of the non-woody tundra and change of suitability also barely contributed to explaining the pattern of shrub expansion (Extended Data Fig. 4). These results suggest environmental suitability was not the major limiting factor of shrub expansion between 1984 and 2014.

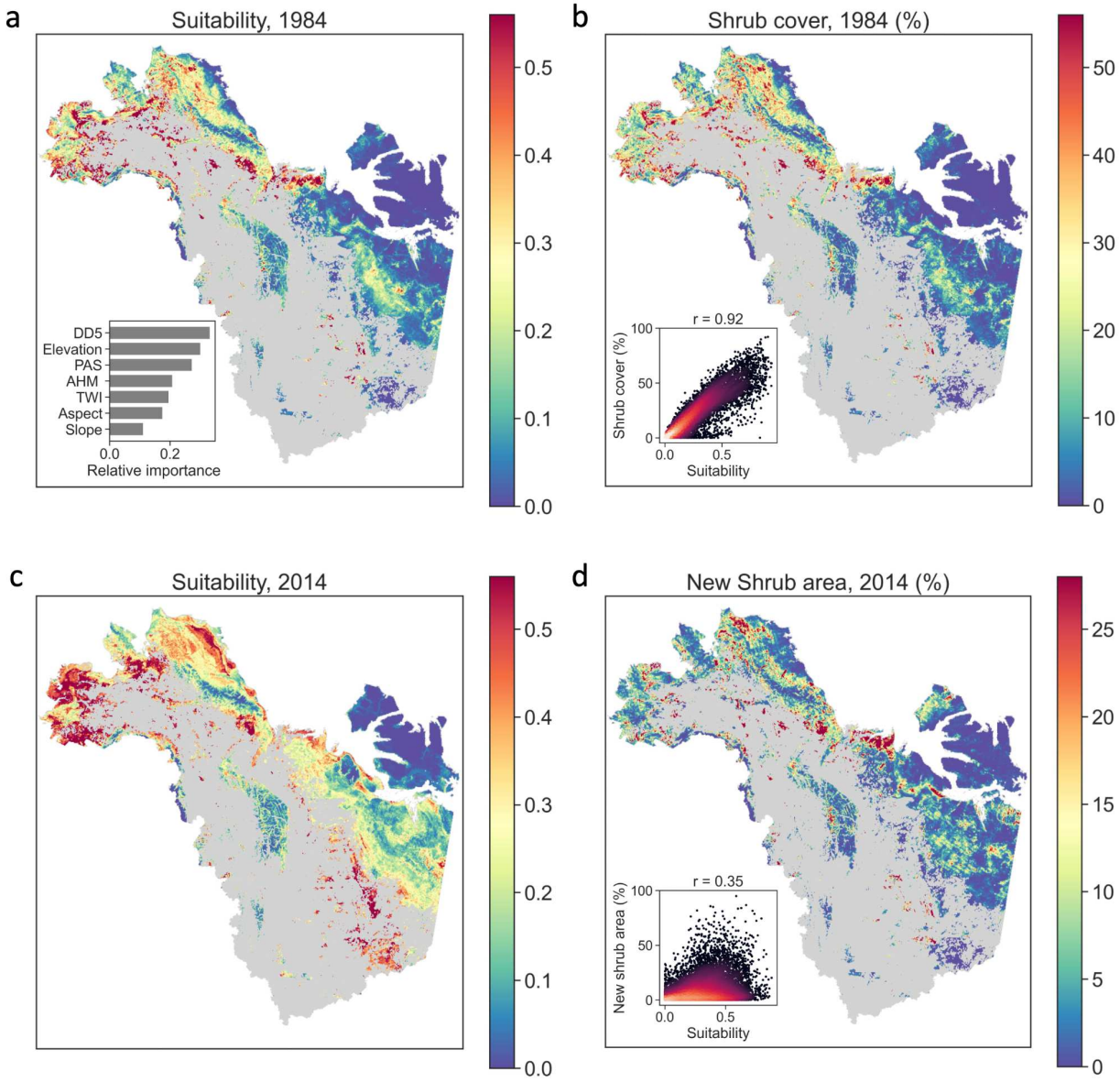

Fig. 1 | Suitability did not explain shrub expansion between 1984 and 2014. Suitability of shrubs in (a) 1984 and (c) 2014 estimated using topographic and bioclimatic conditions, including annual degree-days above 5°C (DD5), annual degree precipitation as snow (PAS), annual heat-moisture index (AHM), elevation, slope, aspect, and topographic wetness index (TWI). The inset of (a) shows the relative importance of these factors on suitability. (b) Fraction of shrub cover in 1984. (d) Fraction of new shrub area in 2014, i.e., non-shrub tundra in 1984

141 that became dominated by shrubs by 2014. The insets of (b) and (d) show the corresponding
142 relationships with suitability, where brighter colors represent higher dot density.
143
144 **Impacts of seed dispersal and fire**
145 The best-fitting long-distance dispersal was represented using a flat-tail kernel (c = 0.5 in Eq. 1
146 in Methods) with a range parameter of 39 km (Extended Data Fig. 5); and the short-distance
147 dispersal was best represented using an exponential power kernel (c = 1.5 in Eq. 1 in Methods),
148 which is between an exponential kernel and a Gaussian kernel and has a range parameter of 600
149 m. Notably, in regions not disturbed by fire, the area fraction of shrub expansion was the most
150 sensitive to short-distance dispersal, 9.5 times more sensitive than to suitability based on the
151 regression coefficients (Fig. 2a). The weak negative sensitivity to long-distance dispersal likely
152 arose from the trade-off between the sensitivities to short- and long-distance dispersal, which
153 might not be precisely separated based on the data due to their spatial correlation (r = 0.71).
154 However, both long- and short-distance dispersal became significantly more important in
155 facilitating shrub expansion after fire, compared to areas without fire (Fig. 2a). The median of
156 the sensitivities to long- and short-distance dispersal increased from -0.010 to 0.029 and from
157 0.062 to 0.083, respectively, for areas that experienced fire; whereas the sensitivity to suitability
158 reduced from 0.006 to -0.007. Across the entire domain, fire disturbance enhanced the likelihood
159 of shrub expansion, especially in highly suitable areas with high seed arrival probability (Fig.
160 2b). Accounting for seed arrival probability and suitability improved the estimation accuracy of
161 shrub expansion from r = 0.35 (Fig. 1d) to r = 0.61 (areas with fire) and r = 0.71 (areas without
162 fire) (Fig. 2b). These findings show that, over recent decades, dispersal has been a stronger
163 limiting factor than suitability on shrub expansion. Non-woody tundra locations becoming more

suitable is not sufficient for shrub expansion to occur. By contrast, fire disturbance and proximity to existing shrub patches make shrub expansion more likely in the newly suitable areas.

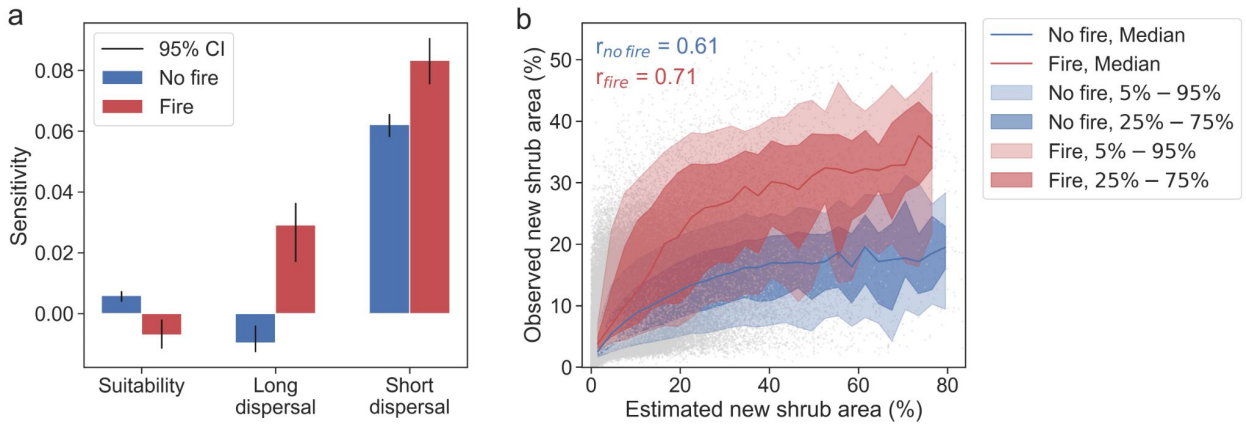

Fig. 2 | Dispersal and fire explain shrub expansion during 1984-2014. (a) Sensitivity of new shrub area to suitability and probabilities of seed arrival via short- and long-distance dispersal at locations with (red bars) and without (blue bars) fire. Vertical black lines denote the range of the 95% confidence interval of the regression coefficients across optimal dispersal kernel parameters. (b) Observed and estimated new shrub area in 2014 at locations with (red) and without (blue) fire. The lines and shaded bands represent the medians and ranges of observed new shrub area (grey dots) for each bin of estimates with a width of 2%.

Predicted shrub expansion

Across the domain, 6.8% of non-shrub tundra in 1984 had become dominated by shrubs by 2014. Using our established relationships (Fig. 2), we estimated that the shrubified area fraction would increase progressively to 25.1% ± 3.0% by 2100 (Fig. 3a, Extended Data Fig. 6) corresponding to 253,651 ± 30,317 km^2 more shrub cover than in 2014, with the uncertainty originating from uncertainty in the empirically derived sensitivities (Fig. 2a). The results suggest substantial shrub expansion in southwestern Alaska, southern and eastern Seward Peninsula, south and north of

182 the Brooks Range, and northern Northwest Territories of Canada. The Victoria Island, western
183 Nunavut, the Brooks Range, and the Mackenzie Mountains will likely experience limited shrub
184 expansion. Note that projected shrub expansion estimated here originates from the combined
185 impacts of suitability under projected climate change, seed dispersal, and projected burn area.
186 The resulting pattern (Fig. 3a) does not account for shrub loss due to competition, pests, and
187 herbivores, which requires future work to better characterize loss mechanisms. By contrast,
188 without considering the impact of dispersal and fire, the relationship between shrub presence and
189 increased suitability alone (Fig. 1a, b) predicts a higher fraction (38.9%) of non-shrub tundra in
190 1984 will become shrublands by 2100. Notably, the shrub expansion pattern predicted using
191 suitability alone shows substantial increase of shrub cover in the North Slope and northern
192 Canada (Fig. 3b), which is significantly different from the expansion if dispersal and fire
193 limitations are considered (Fig. 3a). Thus, relying on environmental suitability alone likely
194 results in predictions that overestimate shrub expansion and misrepresent the spatial patterns. As
195 a result, observational studies and models that project shrub expansion without considering the
196 biological and physical constraints of dispersal and fire likely overestimate the 21st century
197 carbon sink in Arctic tundra due to shrub responses to warming.

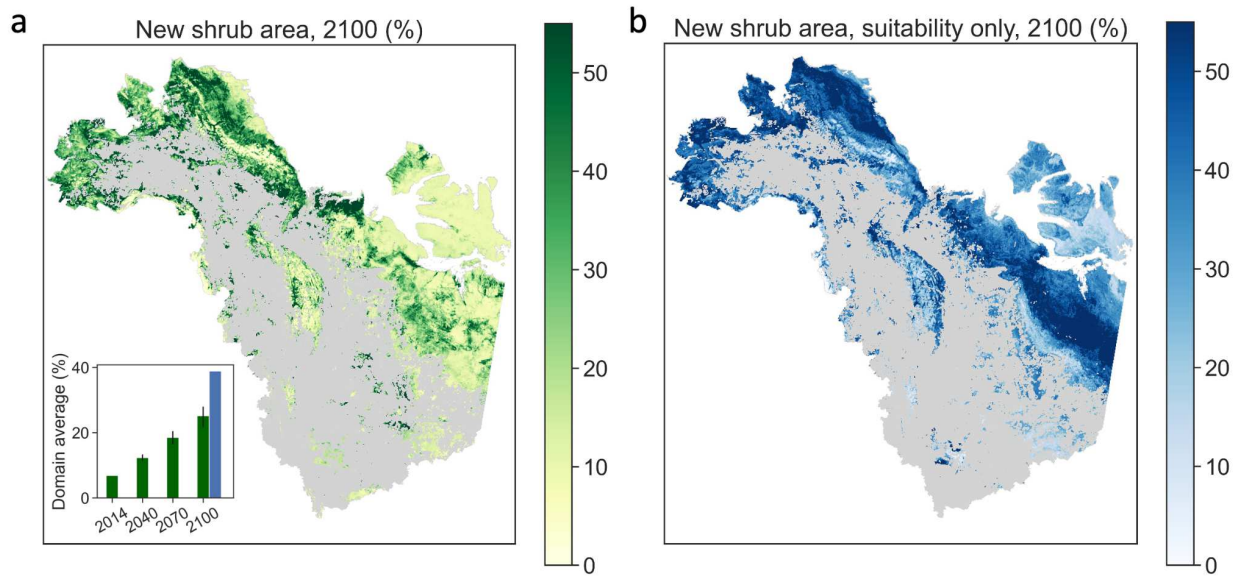

Fig. 3 | A quarter of non-woody tundra in 1984 will be colonized by shrubs by 2100. Spatial pattern of new shrub area in 2100 predicted using (a) suitability, dispersal and fire, and (b) suitability alone. The inset of (a) shows the domain average of new shrub area predicted with (green bars) and without (blue bar) considering dispersal and fire. The vertical black lines illustrate the uncertainty due to uncertainty of the estimated sensitivities, i.e., vertical black lines in Fig. 2a. Using suitability alone overestimates shrub expansion and misrepresents the spatial pattern.

Relative impact of suitability, fire, and dispersal

We investigated the spatial patterns of projected changes in suitability, burn area, and seed arrival probability in 2100, and used synthetic scenarios, i.e., turning-off on factor at a time, to disentangle their individual impacts on projected shrub expansion shown in Fig. 3 (see Methods). Compared to 1984, suitability in 2100 increased in most of the region due to climate warming, although it decreased in some low elevation areas experiencing reduced snow inputs (Extended Data Fig. 7a). Suitability change had a spatially heterogeneous impact on shrub expansion, i.e.,

increasing in most areas but decreasing in parts of southwestern Alaska, the North slope, and northern Canada. Given the low sensitivity of shrub expansion to suitability (Fig. 2a) and the spatial compensation, the net result of suitability changes was small averaged across the region (~1%) by 2100. Fires burned 3.2% of the area during 1984-2014, which was projected to increase to 7% during 2070-2100 based on the CMIP6 ensemble average. Burn area in CMIP6 models was mostly concentrated in the southeast (Extended Data Fig. 7b), which had limited impact on shrub expansion due to low initial shrub cover and thus seed arrival probability in that region (Extended Data Fig. 7c). In the majority of Alaska and northern Canada the burn area was projected to be close to zero until the end of the 21st century. As a result, although areas disturbed by fire were found more likely to experience shrub expansion (Fig. 2), projected fire only contributed one percentage point out of the 25% shrub expansion by 2100, equivalent to the impact of projected suitability change (Fig. 4b). The spatial pattern of seed arrival probability mostly followed existing shrub cover, i.e., high in the majority of Alaska and middle of the Northwest Territories in Canada, and low in coastal regions of Alaska, and southeast and north of the Northwest Territories (Extended Data Fig. 7c). Dispersal largely explained shrub expansion in these regions (Fig. 4c). Notably, although the Brooks Range had moderate seed arrival probability (Extended Data Fig. 7c), shrubs were found unlikely to expand into this region (Fig. 3) due to the limitation of low suitability (Fig. 1c, Extended Data Fig. 7), highlighting the compound impact of suitability and seed dispersal. Across the domain, seed dispersal explained 14% out of the 25% shrubified tundra from 1984 to 2100 (Fig. 4c). Given the dominant control of seed dispersal on the spatial pattern of shrub expansion, omitting dispersal likely leads to mis-represented shrub cover change.

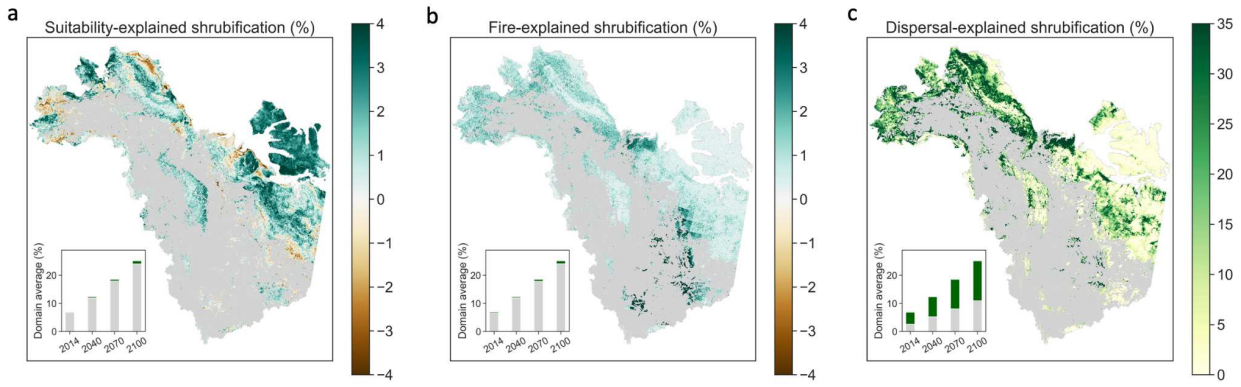

Fig 4 | Shrub expansion over the 21st century was primarily attributed to seed dispersal. Shrub expansion driven by (a) suitability change from 2014 to 2100, (b) projected fire and (c) short- and long-distance seed dispersal. The insets show the domain average of shrub expansion from 2014 to 2100; the grey sections show shrub expansion in a scenario where the corresponding factor was turned off and the green sections represent its contribution.

Discussion and implications

Climate warming has made the Arctic tundra substantially more suitable for shrubs over recent decades. However, we demonstrate that more suitable areas do not necessarily experience more extensive shrub expansion, which, instead, is found in areas close to existing shrub patches and/or disturbed by fire. In contrast to previous findings that suggest a stronger limitation of environmental suitability than seed dispersal over the past millennia[39], the results here indicate dispersal processes limit shrub expansion over recent decades. Our findings provide observational evidence for the importance of seed dispersal in Arctic shrub expansion under rapid warming as the ecosystem deviates from its historical equilibrium. The fact that shrubs did not expand into all suitable areas implies shrub establishment might not have kept up with the pace of recent climate change. In the scenario where suitability is kept the same as in 2014 through 2100, shrub cover is still predicted to substantially increase across the domain (grey bars

255 in Fig. 4a). Therefore, shrubs will likely continue to expand across the Arctic tundra, even under
256 a net-zero emission scenario, where global warming will be limited to 1.5 °C by 2050 and
257 stabilized by 2100[50].

258 Complex ecosystem processes introduce uncertainties in predicted suitability, identified
259 shrub expansion, and the relationship to seed dispersal and fire disturbance. Uncertainties related
260 to future suitability can be influenced by future bioclimatic conditions exceeding the historical
261 ranges used to establish their relationships with suitability (Extended Data Fig. 8). For example,
262 nutrient availability could increase much faster with temperature in a warmer climate due to an
263 exponential increase of N mineralization rate and deepening active layer[43]. Thus, the data-driven
264 suitability model trained using historical data could underestimate future suitability. However,
265 mechanistic models could contribute to addressing such uncertainties. Shrub expansion was
266 identified based on remotely-sensed shrub dominance at a 30 m scale and over 30 years[3],
267 therefore it may not precisely distinguish the underlying causes of seed dispersal and emergence
268 of pre-existing shrubs[3,9]. However, because shrub emergence is expected to be controlled by
269 environmental suitability, the low impact of suitability supports seed dispersal being the
270 dominant cause of shrub expansion across the domain. Moreover, as dispersal is estimated based
271 on spatial proximity, our results highlight the importance of spatially connected processes.
272 Although seed dispersal is the originating mechanism and has been recognized as a dominant
273 spatial process controlling vegetation range shifts[33–37], the impact of spatial proximity identified
274 here might also be partially attributed to other spatially connected factors, such as active layer
275 depth, soil thermal-hydro conditions, surface litter, nutrient availability, and herbivore
276 activities[51–54]. These factors may contribute to the spatial connectivity of shrub expansion via
277 rates of seed germination and seedling establishment. However, these factors are unlikely to be

the dominant explanation for the identified impact of spatial proximity, as they are partially related to suitability via climate and topographic conditions, and they tend to exhibit smaller spatial ranges than those identified for long-distance dispersal (~40 km). Field surveys and measurements are required to investigate the confounding roles of these spatial processes.

Although fires can either enhance or inhibit plant regeneration depending on local soil and climate conditions[25], our results suggest fire enhances shrub expansion where it does occur, consistent with palaeoecological studies[42] and model simulations[43,55] across a large scale. The strong compounding effect of fire and seed dispersal on shrub expansion (Fig. 2) highlights that fire promotes shrub expansion especially at locations close to preexisting shrub patches, where seeds are more likely to arrive and establish after fire. Because fire is projected to be rare in the Arctic tundra based on climate models, we find it only marginally contributes to shrub expansion by 2100. However, a recent study suggests lightning in Arctic tundra, the dominant source of burning[56], will significantly increase to a rate similar to that in boreal forests[16]. Lightning-driven fire increases could trigger positive vegetation-fire feedbacks, leading to twofold more burn area by 2100 than the ensemble average of CMIP6 models (Extended Data Fig. 9)[16,57]. Therefore, fire likely exerts greater impacts on shrub expansion compared to the estimates here when considering these positive feedbacks, though further investigation is required to constrain the large uncertainty (Extended Data Fig. 9). As post-fire regeneration strongly controls how much fire-induced carbon loss is attenuated[17], future work on the strength and spatial heterogeneity of the feedback between fire and shrub expansion will contribute to a better assessment of carbon budget in Arctic tundra.

Our results highlight that predicting shrub expansion cannot be based on climate alone. Models that do not account for fire disturbance and seed dispersal may misrepresent future shrub

301 cover. In Earth system models, seed production and dispersal have been recognized as the most
302 under-developed vegetation demographic processes[58]. Representing seed dispersal, especially
303 over long distances, requires seed transport across spatially discretized grids, which does not
304 exist in most land models. Improved representation of seed dispersal therefore could contribute
305 to better prediction of vegetation shifts. In addition to the factors investigated here, shrub
306 expansion is also modulated by species competition for water, nutrients, and light[59–61]. Recent
307 observational evidence suggests climate change can result in different competitive abilities
308 across species due to divergent shifts of plant functional traits in Arctic tundra[62–64], highlighting
309 the potential of employing dynamic vegetation models that explicitly represent competition.
310 These findings motivate improving process-based representations of seed dispersal, fire
311 disturbance, and species competition in dynamic vegetation models as a fundamental component
312 to better prediction of Arctic shrub change and corresponding climate feedbacks.

Methods

Datasets

Shrub expansion was identified based on the Landsat-derived product of annual dominant land cover across ABoVE core domain from 1984 to 2014[65]. The dataset provides annual dominant plant functional type at a 30 m resolution derived from Landsat surface reflectance, very high resolution imagery, and field photography across the ABoVE domain. We focused on pixels dominated by shrubs and non-woody species, i.e., excluding boreal forests. Pixels consistently classified as shrublands during 1984-1986 and 2012-2014 were considered as shrub cover in 1984 and 2014, minimizing the uncertainty of noise in annual time series of land cover types. New shrub area was identified as pixels that had been dominated by non-woody species in 1984 and became dominated by shrubs in 2014. We used climate and topographic conditions to estimate environmental suitability for shrublands. The climate conditions came from ClimateNA[66], a product locally downscaled for North America at a 4 km resolution. The historical data (1955-2014) was downscaled from the gridded Climatic Research Unit Time-series data version 4.02 (CRU TS4.02), and the projected data (2014-2100) was downscaled from CMIP5 under the RCP8.5 scenario. The elevation data was obtained from the Advanced Spaceborne Thermal Emission and Reflection Radiometer (ASTER) Global Digital Elevation Model Version 3 with a 30 m resolution[67]. Slope, aspect, and the topographic wetness index were derived from elevation using a terrain analysis software RichDEM[68]. Fire occurrence during 1985-2009 was identified using the annual product of differenced Normalized Burned Ratio (dNBR) at a 30 m resolution[69], where the perimeters came from the Alaskan Interagency Coordination Center and the Natural Resources Canada fire occurrence datasets. Only fires that occurred at least 5 years prior to 2014 were considered to allow vegetation recovery. Burn area

during 2015-2100 was obtained from CMIP6 projections under a SSP585 scenario. Datasets at coarse resolutions (climate and projected burn area) were resampled to a 30 m resolution using the nearest neighbour method.

Estimation of environmental suitability

We considered 23 bioclimatic variables (Extended Data Table 1) and 4 topographic conditions, i.e., elevation, slope, aspect, and topographic wetness index. To reduce the risk of overfitting, we identified the most informative variables based on the variance inflation factor, which measures the multicollinearity among the explanatory variables. Starting from all 27 variables, we excluded the variable with the highest variance inflation factor, i.e., the variable that can be best represented by a linear combination of other variables, one at a time, until the variance inflation factors of all variables are below the commonly used threshold of five[70]. This procedure ensured that the identified variables are most statistically informative in representing the bioclimatic and topographic conditions across the domain. Based on the identified variables, we applied 10 species distribution models to estimate whether a pixel was shrubland. The models include generalized linear model, generalized additive model, boosted regression trees, classification tree analysis, artificial neural network, surface range envelope, flexible discriminant analysis, multiple adaptive regression splines, random forest, and maximum entropy, all applied using the *biomod2*[71] software in R[72]. Due to the large computation load, we trained each model using 5% of the pixels randomly selected within the target area, including both shrub and non-shrub pixels. The model accuracies were evaluated using all pixels across the entire domain. The random forest model had the highest accuracy based on the true skill statistic and the area under the receiver operating characteristic curve. Therefore, the environmental suitability, i.e., the

probability of a given 30 m pixel being shrubland given its bioclimatic and topographic conditions, was calculated using only the random forest model. We assumed a relatively stable climate prior to 1984. Thus, the average bioclimatic conditions during 1955-1984 were used to train the random forest model and assess suitability in 1984. Suitability in 2014, 2040, 2070, and 2100 were estimated by replacing the bioclimatic conditions to the averages over the previous 30 years, respectively. We evaluated the relative importance of each variable in explaining suitability. We also analyzed the response curve of suitability to the variation of each variable, and the response surfaces to the covariation of the most important three variables, while setting other variables as the domain average.

Seed arrival probability

The impact of seed dispersal was quantified using the probability of seed arrival at a given location, calculated using kernel convolution over the spatial pattern of shrublands. The following exponential power kernel was used to describe the relationship between seed arrival probability and distance to parent shrub patches.

$$k(x_i) = \frac{b}{2\pi a^2 \Gamma(2/b)} \exp\left(-\left(\frac{x_i}{a}\right)^b\right) \quad (1)$$

where x_i is the distance to the ith shrubland pixel within a maximum range, which is considered as the distance where the kernel function first falls below 10^{-9}; a and b are the range and shape parameters, respectively. Large a represents high seed arrival probability from distant parent shrub patches and vice versa. Large b denotes a fast decay rate of seed arrival probability with distance and vice versa. The exponential power kernel is a generalized form of the Gaussian (b = 2), exponential (b = 1), and flat-tailed (b = 0.5) kernels, and has been widely used in literature[73]. The seed arrival probability of a given location (s) is calculated as follows:

$$p(s) = \frac{1}{P_{\max}} \sum_{i=1}^{N} k(x_i)\Delta x \quad (2)$$

where N is the total number of shrub pixels within the maximum range; $\Delta x = 30$ m is the width of a pixel; and $P_{\max}$ is the normalization factor such that $p(s) = 1$when the location is completely surrounded by shrublands within the maximum range. The seed arrival probability $p(s)$ measures the spatial proximity to existing shrublands. Assuming the same seed production of all shrublands, the seed arrival probability $p(s)$is also proportional to the expectation of the arriving seed amount. Based on the shrub cover in 1984, we calculated the seed arrival probability during 1984-2014 using the above described algorithm implemented in the multidimensional image processing software of *scipy.ndimage*[74]. To account for various dispersal vectors[32], we considered both short-distance and long-distance dispersal kernels. For short-distance dispersal, we evaluated all combinations of 100 m$\leq a \leq$1000 m with an interval of 100 m and $0.5 \leq b \leq 2.5$with an interval of 0.5. For long-distance dispersal, we evaluated all combinations of 1 km$< a \leq$60 km with an interval of 2 km and $0.5 \leq b \leq 2.5$with an interval of 0.5. We identified the parameters that resulted in the best 5% accuracy in estimating shrub expansion during 1984-2014.

Sensitivity of observed shrub expansion to control factors

Observed shrub expansion was quantified as the fraction of 30 m pixels that were not identified as shrublands in 1984, i.e., non-shrub tundra, but became shrublands in 2014 within each 4 km by 4 km gridcell. Suitability and seed arrival probabilities through short- and long-distance dispersal were aggregated by average to a 4 km scale and used to explain the spatial pattern of shrub expansion using multivariate linear regression. We calculated the regression accuracy and the sensitivities (regression coefficients) to the z-scores of the explanatory variables for gridcells

405 with and without fire occurrence, respectively. The 95% confidence intervals of the sensitivities
406 were estimated.
407
408 **Prediction of shrub expansion by 2100**
409 Based on the estimated empirical relationships, we predicted shrub expansion by 2040, 2070, and
410 2100. For each 30-year period, suitability was estimated using topographic conditions and the
411 averages of projected bioclimatic conditions. Seed arrival probability was estimated using shrub
412 cover at the start of the period. Fire was assigned for each 30 m pixel with a probability
413 represented by the cumulative burn area fraction, ensuring the aggregation from a 30 m scale
414 consistent with the climate model projection at a coarser scale. Each non-shrub pixel at the start
415 of the 30-year period was changed to shrubland at the end with a probability calculated using the
416 estimated sensitivities to its suitability, seed arrival probability, and fire occurrence. We further
417 quantified the uncertainty of projected shrub expansion due to the uncertainty in the estimated
418 sensitivities. Instead of a computationally expensive bootstrapping approach, we used the lower
419 and upper boundaries of the 95% confidence intervals for all the regression coefficients in each
420 30-year period, which provided an overestimate of the uncertainty range of projected shrub
421 expansion. To disentangle the impacts of suitability change, seed dispersal, and fire on the
422 projected shrub expansion, we used synthetic scenarios where each of the three factors was
423 turned off, i.e., suitability kept the same as in 2014, zero seed arrival probability, and no fire
424 occurrence, respectively. The difference between the synthetic scenarios and the actual
425 projection illustrated the contribution of the corresponding factor on the projected shrub
426 expansion. To diagnose potential bias and spatial patterns of predicted shrub expansion using the
427 suitability-based approach in previous studies, the shrub expansion by 2100 predicted here was

also compared to the prediction without considering dispersal and fire, i.e., by applying 2100 suitability to the relationship established between shrub presence and suitability alone in 1984.

References

1. Post, E. *et al.* The polar regions in a 2°C warmer world. *Sci Adv* **5**, eaaw9883 (2019).
2. Pearson, R. G. *et al.* Shifts in Arctic vegetation and associated feedbacks under climate change. *Nat. Clim. Chang.* **3**, 673–677 (2013).
3. Wang, J. A. *et al.* Extensive land cover change across Arctic-Boreal Northwestern North America from disturbance and climate forcing. *Glob. Chang. Biol.* **26**, 807–822 (2020).
4. Mekonnen, Z. A. *et al.* Arctic tundra shrubification: a review of mechanisms and impacts on ecosystem carbon balance. *Environ. Res. Lett.* **16**, 053001 (2021).
5. Elmendorf, S. C. *et al.* Plot-scale evidence of tundra vegetation change and links to recent summer warming. *Nat. Clim. Chang.* **2**, 453–457 (2012).
6. Sturm, M., Racine, C. & Tape, K. Climate change. Increasing shrub abundance in the Arctic. *Nature* **411**, 546–547 (2001).
7. Tape, K., Sturm, M. & Racine, C. The evidence for shrub expansion in Northern Alaska and the Pan-Arctic. *Glob. Chang. Biol.* **12**, 686–702 (2006).
8. Forbes, B. C., Fauria, M. M. & Zetterberg, P. Russian Arctic warming and 'greening' are closely tracked by tundra shrub willows. *Glob. Chang. Biol.* **16**, 1542–1554 (2010).
9. Myers-Smith, I. H. *et al.* Complexity revealed in the greening of the Arctic. *Nat. Clim. Chang.* **10**, 106–117 (2020).
10. Chapin, F. S., 3rd *et al.* Role of land-surface changes in arctic summer warming. *Science* **310**, 657–660 (2005).

11. Swann, A. L., Fung, I. Y., Levis, S., Bonan, G. B. & Doney, S. C. Changes in Arctic vegetation amplify high-latitude warming through the greenhouse effect. *Proc. Natl. Acad. Sci. U. S. A.* **107**, 1295–1300 (2010).
12. Bonfils, C. J. W. *et al.* On the influence of shrub height and expansion on northern high latitude climate. *Environ. Res. Lett.* **7**, 015503 (2012).
13. Natali, S. M. *et al.* Large loss of CO2 in winter observed across the northern permafrost region. *Nat. Clim. Chang.* **9**, 852–857 (2019).
14. Paradis, M., Lévesque, E. & Boudreau, S. Greater effect of increasing shrub height on winter versus summer soil temperature. *Environ. Res. Lett.* **11**, 085005 (2016).
15. Post, E. *et al.* Ecological dynamics across the Arctic associated with recent climate change. *Science* **325**, 1355–1358 (2009).
16. Chen, Y. *et al.* Future increases in Arctic lightning and fire risk for permafrost carbon. *Nat. Clim. Chang.* 1–7 (2021) doi:10.1038/s41558-021-01011-y.
17. Mack, M. C. *et al.* Carbon loss from boreal forest wildfires offset by increased dominance of deciduous trees. *Science* **372**, 280–283 (2021).
18. Keenan, T. F. & Riley, W. J. Greening of the land surface in the world's cold regions consistent with recent warming. *Nat. Clim. Chang.* **8**, 825–828 (2018).
19. Büntgen, U. *et al.* Temperature-induced recruitment pulses of Arctic dwarf shrub communities. *J. Ecol.* **103**, 489–501 (2015).
20. Myers-Smith, I. H. & Hik, D. S. Climate warming as a driver of tundra shrubline advance. *J. Ecol.* **106**, 547–560 (2018).
21. Tape, K. D., Hallinger, M., Welker, J. M. & Ruess, R. W. Landscape Heterogeneity of Shrub Expansion in Arctic Alaska. *Ecosystems* **15**, 711–724 (2012).

22. Myers-Smith, I. H. *et al.* Climate sensitivity of shrub growth across the tundra biome. *Nat. Clim. Chang.* **5**, 887–891 (2015).
23. Berner, L. T. *et al.* Summer warming explains widespread but not uniform greening in the Arctic tundra biome. *Nat. Commun.* **11**, 4621 (2020).
24. Campbell, T. K. F., Lantz, T. C., Fraser, R. H. & Hogan, D. High Arctic Vegetation Change Mediated by Hydrological Conditions. *Ecosystems* **24**, 106–121 (2021).
25. Chen, Y., Hu, F. S. & Lara, M. J. Divergent shrub-cover responses driven by climate, wildfire, and permafrost interactions in Arctic tundra ecosystems. *Glob. Chang. Biol.* **27**, 652–663 (2021).
26. Martin, A. C., Jeffers, E. S., Petrokofsky, G., Myers-Smith, I. & Macias-Fauria, M. Shrub growth and expansion in the Arctic tundra: an assessment of controlling factors using an evidence-based approach. *Environ. Res. Lett.* **12**, 085007 (2017).
27. Blois, J. L., Williams, J. W., Fitzpatrick, M. C., Jackson, S. T. & Ferrier, S. Space can substitute for time in predicting climate-change effects on biodiversity. *Proc. Natl. Acad. Sci. U. S. A.* **110**, 9374–9379 (2013).
28. Svenning, J.-C. & Sandel, B. Disequilibrium vegetation dynamics under future climate change. *Am. J. Bot.* **100**, 1266–1286 (2013).
29. Damgaard, C. A Critique of the Space-for-Time Substitution Practice in Community Ecology. *Trends Ecol. Evol.* **34**, 416–421 (2019).
30. Klesse, S. *et al.* Continental-scale tree-ring-based projection of Douglas-fir growth: Testing the limits of space-for-time substitution. *Glob. Chang. Biol.* **26**, 5146–5163 (2020).
31. Nathan, R. *et al.* Mechanisms of long-distance seed dispersal. *Trends Ecol. Evol.* **23**, 638–647 (2008).

32. Rogers, H. S. *et al.* The total dispersal kernel: a review and future directions. *AoB Plants* **11**, lz042 (2019).
33. Anadon-Rosell, A., Talavera, M., Ninot, J. M., Carrillo, E. & Batllori, E. Seed production and dispersal limit treeline advance in the Pyrenees. *J. Veg. Sci.* **31**, 981–994 (2020).
34. Standish, R. J., Cramer, V. A., Wild, S. L. & Hobbs, R. J. Seed dispersal and recruitment limitation are barriers to native recolonization of old-fields in western Australia. *J. Appl. Ecol.* **44**, 435–445 (2007).
35. Kunstler, G. *et al.* Tree colonization of sub-Mediterranean grasslands: effects of dispersal limitation and shrub facilitation. *Can. J. For. Res.* **37**, 103–115 (2007).
36. Reid, J. L., Holl, K. D. & Zahawi, R. A. Seed dispersal limitations shift over time in tropical forest restoration. *Ecol. Appl.* **25**, 1072–1082 (2015).
37. van Breugel, M. *et al.* Soil nutrients and dispersal limitation shape compositional variation in secondary tropical forests across multiple scales. *J. Ecol.* **107**, 566–581 (2019).
38. Münzbergová, Z. & Herben, T. Seed, dispersal, microsite, habitat and recruitment limitation: identification of terms and concepts in studies of limitations. *Oecologia* **145**, 1–8 (2005).
39. Alsos, I. G. *et al.* Frequent long-distance plant colonization in the changing Arctic. *Science* **316**, 1606–1609 (2007).
40. Makoto, K. & Wilson, S. D. When and where does dispersal limitation matter in primary succession? *J. Ecol.* **107**, 559–565 (2019).
41. Flannigan, M., Stocks, B., Turetsky, M. & Wotton, M. Impacts of climate change on fire activity and fire management in the circumboreal forest. *Glob. Chang. Biol.* **15**, 549–560 (2009).

42. Higuera, P. E. *et al.* Frequent fires in ancient shrub tundra: implications of paleorecords for arctic environmental change. *PLoS One* **3**, e0001744 (2008).
43. Mekonnen, Z. A., Riley, W. J., Randerson, J. T., Grant, R. F. & Rogers, B. M. Expansion of high-latitude deciduous forests driven by interactions between climate warming and fire. *Nat Plants* **5**, 952–958 (2019).
44. Johnstone, J. F., Hollingsworth, T. N., Chapin, F. S., III & Mack, M. C. Changes in fire regime break the legacy lock on successional trajectories in Alaskan boreal forest. *Glob. Chang. Biol.* **16**, 1281–1295 (2010).
45. Bret-Harte, M. S. *et al.* The response of Arctic vegetation and soils following an unusually severe tundra fire. *Philos. Trans. R. Soc. Lond. B Biol. Sci.* **368**, 20120490 (2013).
46. Klupar, I., Rocha, A. V. & Rastetter, E. B. Alleviation of nutrient co-limitation induces regime shifts in post-fire community composition and productivity in Arctic tundra. *Glob. Chang. Biol.* **27**, 3324–3335 (2021).
47. Racine, C., Jandt, R., Meyers, C. & Dennis, J. Tundra Fire and Vegetation Change along a Hillslope on the Seward Peninsula, Alaska, U.S.A. *Arct. Antarct. Alp. Res.* **36**, 1–10 (2004).
48. Narita, K. *et al.* Vegetation and Permafrost Thaw Depth 10 Years after a Tundra Fire in 2002, Seward Peninsula, Alaska. *Arct. Antarct. Alp. Res.* **47**, 547–559 (2015).
49. Iwahana, G. *et al.* Geomorphological and geochemistry changes in permafrost after the 2002 tundra wildfire in Kougarok, Seward Peninsula, Alaska. *J. Geophys. Res. Earth Surf.* **121**, 1697–1715 (2016).
50. IPCC. *Global warming of 1.5 C. An IPCC Special Report on the impacts of global warming of 1.5°C above pre-industrial levels and related global greenhouse gas emission pathways, in the context of strengthening the global response to the threat of climate change,*

sustainable development, and efforts to eradicate poverty. (Intergovernmental Panel on Climate Change., 2018).

51. Graae, B. J. *et al.* Strong microsite control of seedling recruitment in tundra. *Oecologia* **166**, 565–576 (2011).
52. Frei, E. R. *et al.* Biotic and abiotic drivers of tree seedling recruitment across an alpine treeline ecotone. *Sci. Rep.* **8**, 10894 (2018).
53. Huebner, D. C. & Bret-Harte, M. S. Microsite conditions in retrogressive thaw slumps may facilitate increased seedling recruitment in the Alaskan Low Arctic. *Ecol. Evol.* **9**, 1880–1897 (2019).
54. Hargreaves, A. L. *et al.* Seed predation increases from the Arctic to the Equator and from high to low elevations. *Sci Adv* **5**, eaau4403 (2019).
55. Rupp, T. S., Starfield, A. M. & Chapin, F. S. A frame-based spatially explicit model of subarctic vegetation response to climatic change: comparison with a point model. *Landsc. Ecol.* **15**, 383–400 (2000).
56. Veraverbeke, S. *et al.* Lightning as a major driver of recent large fire years in North American boreal forests. *Nat. Clim. Chang.* **7**, 529–534 (2017).
57. Camac, J. S., Williams, R. J., Wahren, C.-H., Hoffmann, A. A. & Vesk, P. A. Climatic warming strengthens a positive feedback between alpine shrubs and fire. *Glob. Chang. Biol.* **23**, 3249–3258 (2017).
58. McDowell, N. G. *et al.* Pervasive shifts in forest dynamics in a changing world. *Science* **368**, (2020).
59. Angers-Blondin, S., Myers-Smith, I. H. & Boudreau, S. Plant–plant interactions could limit recruitment and range expansion of tall shrubs into alpine and Arctic tundra. *Polar Biol.* **41**,

2211–2219 (2018).

60. Mekonnen, Z. A., Riley, W. J. & Grant, R. F. Accelerated Nutrient Cycling and Increased Light Competition Will Lead to 21st Century Shrub Expansion in North American Arctic Tundra. *J. Geophys. Res. Biogeosci.* **123**, 1683–1701 (2018).

61. Scherrer, D., Vitasse, Y., Guisan, A., Wohlgemuth, T. & Lischke, H. Competition and demography rather than dispersal limitation slow down upward shifts of trees' upper elevation limits in the Alps. *J. Ecol.* **108**, 2416–2430 (2020).

62. Kunstler, G. *et al.* Plant functional traits have globally consistent effects on competition. *Nature* **529**, 204–207 (2016).

63. Bjorkman, A. D. *et al.* Plant functional trait change across a warming tundra biome. *Nature* **562**, 57–62 (2018).

64. Myers-Smith, I. H., Thomas, H. J. D. & Bjorkman, A. D. Plant traits inform predictions of tundra responses to global change. *New Phytol.* **221**, 1742–1748 (2019).

65. Wang, J. A. *et al.* ABoVE: Landsat-derived Annual Dominant Land Cover Across ABoVE Core Domain, 1984-2014. (2019).

66. Wang, T., Hamann, A., Spittlehouse, D. & Carroll, C. Locally Downscaled and Spatially Customizable Climate Data for Historical and Future Periods for North America. *PLoS One* **11**, e0156720 (2016).

67. NASA/METI/AIST/Japan Spacesystems and U.S./Japan ASTER Science Team. ASTER Global Digital Elevation Model V003. (2019).

68. Barnes, R. RichDEM: Terrain Analysis Software. (2016).

69. Loboda, T. V., Chen, D., Hall, J. V. & He, J. ABoVE: Landsat-derived Burn Scar dNBR across Alaska and Canada, 1985-2015. (2018).

70. James, G., Witten, D., Hastie, T. & Tibshirani, R. *An introduction to statistical learning: With applications in R*. (Springer, 2013). doi:10.1007/978-1-4614-7138-7.
71. Thuiller, W., Georges, D., Gueguen, M., Engler, R. & Breiner, F. *biomod2: Ensemble Platform for Species Distribution Modeling*. https://CRAN.R-project.org/package=biomod2 (2013).
72. R Core Team. *R: A Language and Environment for Statistical Computing*. http://www.R-project.org/ (2013).
73. Bullock, J. M. *et al.* A synthesis of empirical plant dispersal kernels. *J. Ecol.* **105**, 6–19 (2017).
74. Virtanen, P. *et al.* SciPy 1.0: fundamental algorithms for scientific computing in Python. *Nat. Methods* **17**, 261–272 (2020).

Extended Data

Extended Data Table 1 | The Full set of candidate climate variables. Details of each variable were described in Wang et al. (2016).

Variable name and unit
- Mean annual temperature (°C)
- Mean warmest month temperature (°C)
- Mean coldest month temperature (°C)
- Temperature difference between MWMT and MCMT, or continentality (°C)
- Mean annual precipitation (mm),
- May to September precipitation (mm),
- Annual heat-moisture index (MAT+10)/(MAP/1000))
- Summer heat-moisture index ((MWMT)/(MSP/1000))
- Degree-days below 0°C, chilling degree-days
- Degree-days above 5°C, growing degree-days
- Degree-days below 18°C, heating degree-days
- Degree-days above 18°C, cooling degree-days
- Number of frost-free days
- Frost-free period
- The day of the year on which FFP begins
- The day of the year on which FFP ends
- Precipitation as snow (mm). For individual years, it covers the period between August in the previous year and July in the current year.
- Extreme minimum temperature over 30 years
- Extreme maximum temperature over 30 years
- Hargreaves reference evaporation (mm)
- Hargreaves climatic moisture deficit (mm)
- Mean annual solar radiation (MJ m^{-2} d^{-1})
- Mean annual relative humidity (%)

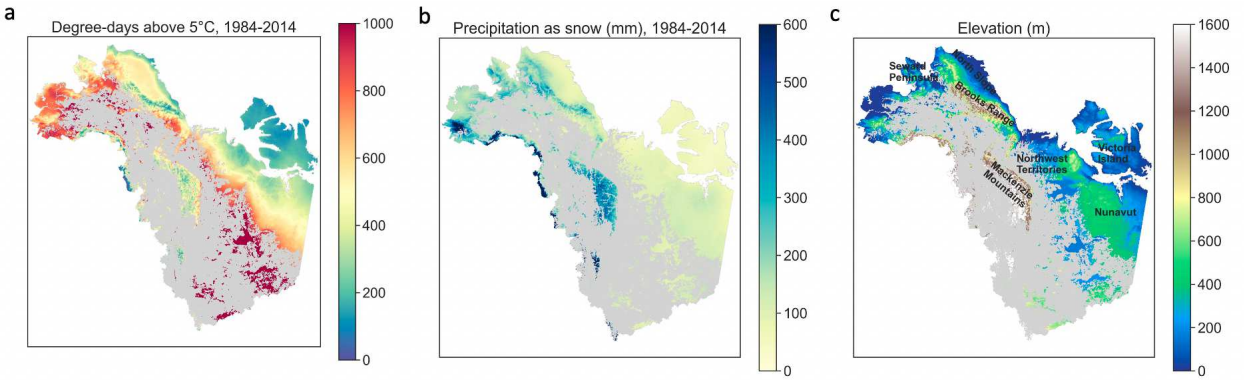

Extended Data Fig. 1 | Spatial patterns of the dominant climate and topographic conditions on environmental suitability. Average (a) degree-days above 5 ℃ and (b) precipitation as snow during 1984-2014. (c) Elevation across the domain, illustrated using a 4 km resolution.

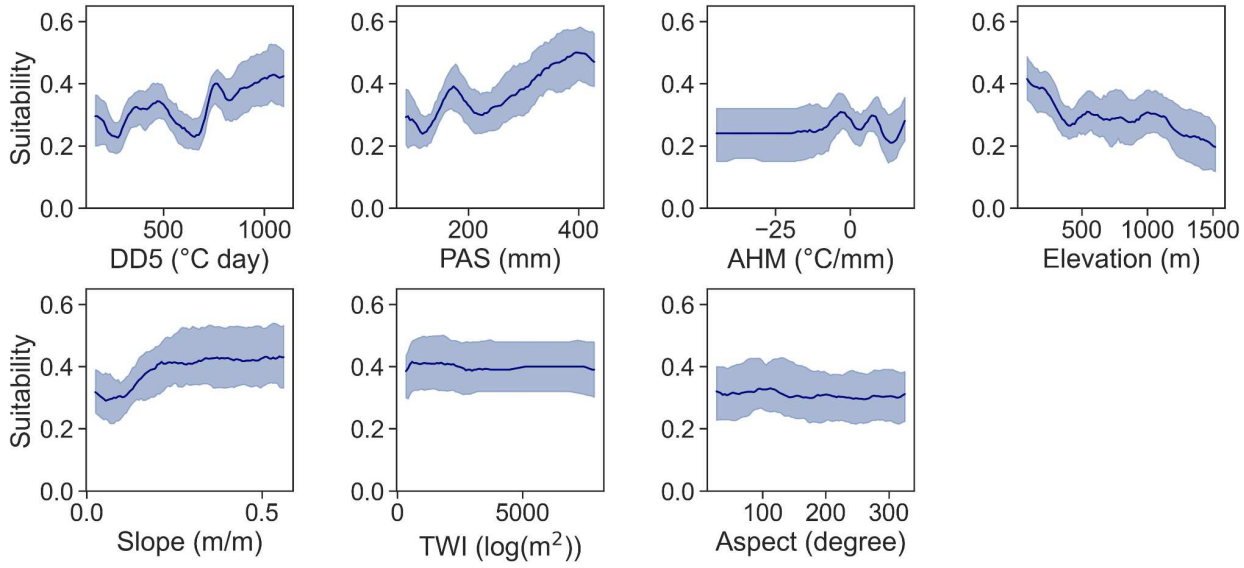

Extended Data Fig. 2 | Response curve of suitability to climate and topographic conditions. The conditions include annual degree-days above 5 ℃ (DD5), annual precipitation as snow (PAS), annual heat-moisture index (AHM), elevation, slope, topographic wetness index (TWI), and aspect. The line and shaded band in each panel show the median and 5%-95% uncertainty range uncertainty across 100 random forest runs.

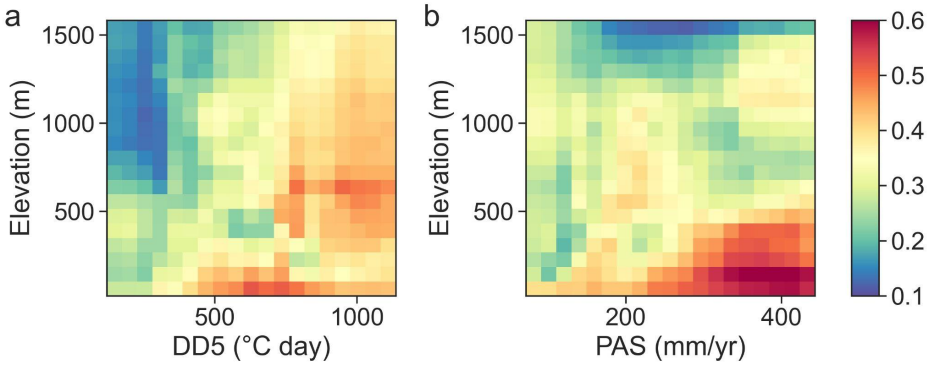

616

617 **Extended Data Fig. 3 | Response surface of suitability to annual degree-days above 5 ℃**

618 **(DD5), annual precipitation as snow (PAS), and elevation.**

619

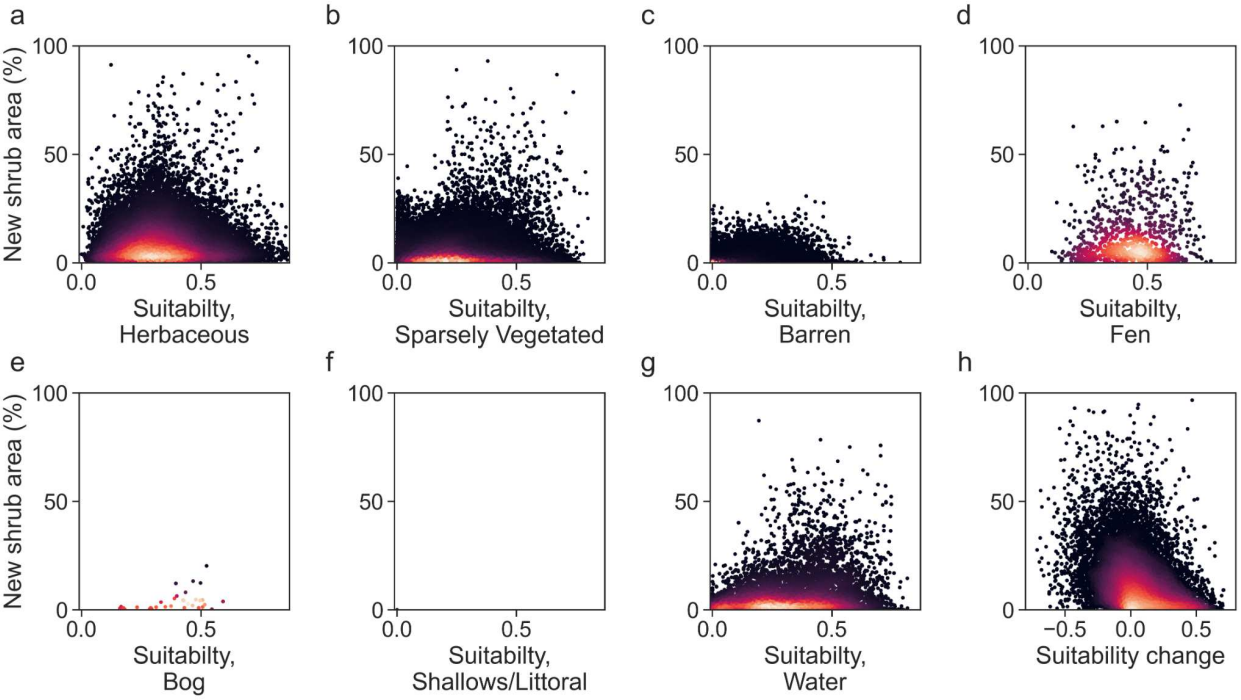

620

621 **Extended Data Fig. 4 | Relationships of new shrub area in 2014 with suitability in different**

622 **initial land cover types in 1984, and with suitability change between 1984-2014.**

623

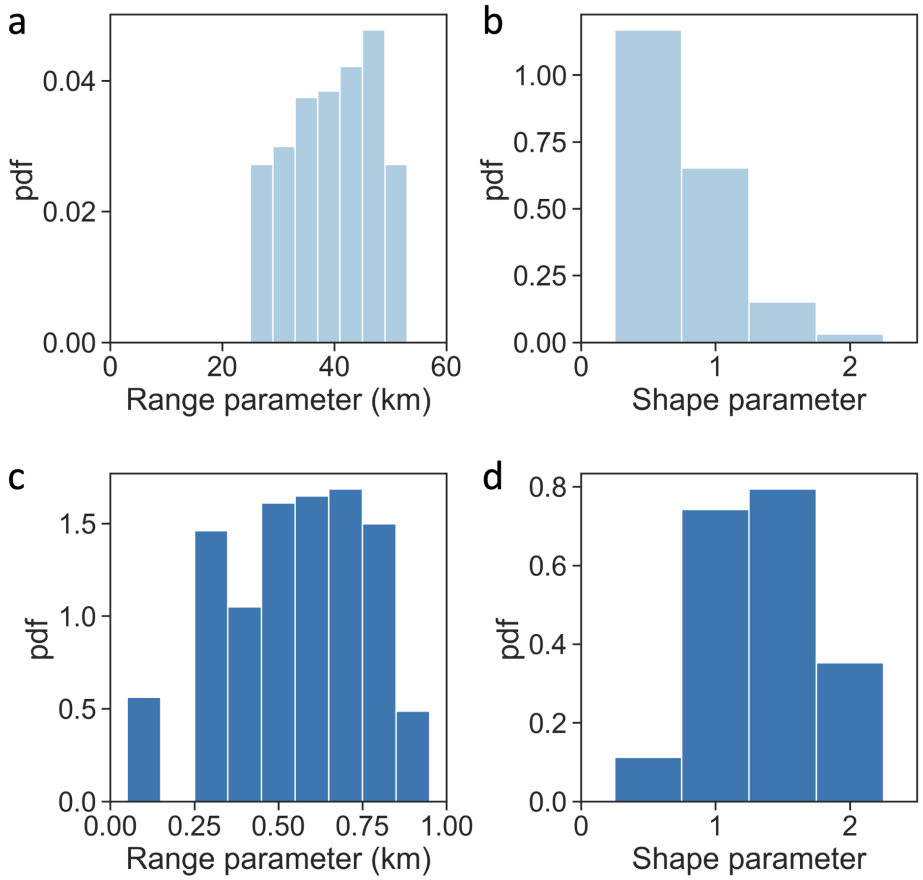

Extended Data Fig. 5 | Probabilistic distributions of the seed dispersal kernel parameters across the top 5% ensembles that match with observation. Parameters of the (a, b) long-distance and (c, d) short-distance dispersal kernels.

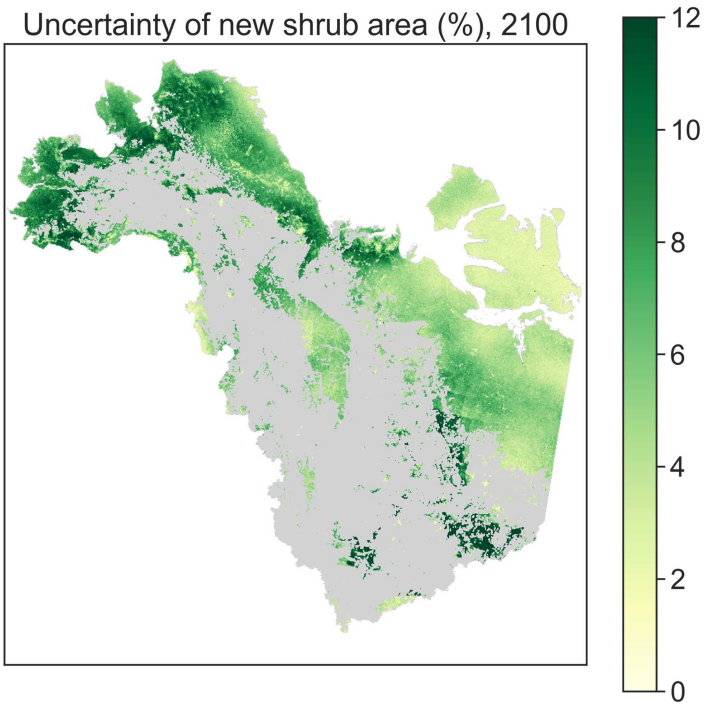

629

630 **Extended Data Fig. 6 | Uncertainty range of estimated new shrub area in 2100.**

631

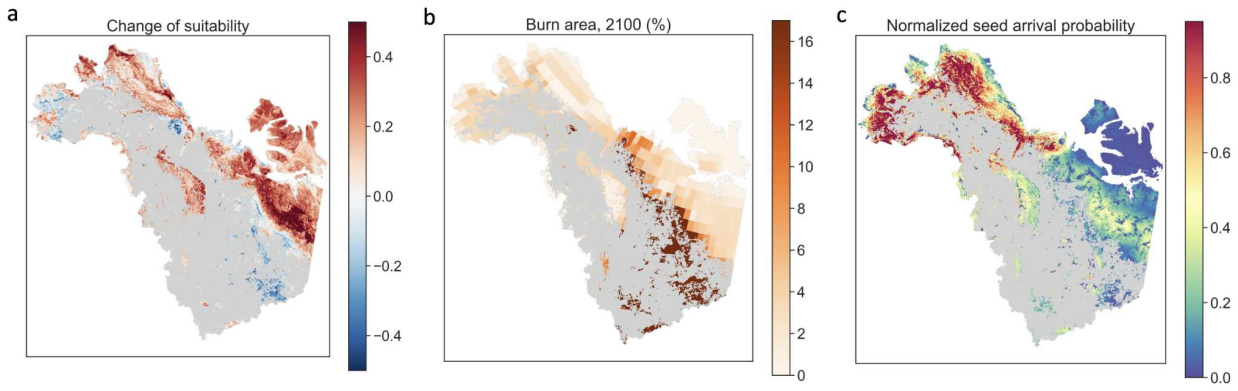

632

633 **Extended Data Fig. 7 | Spatial patterns of suitability change from 2014 to 2100, 30-year**

634 **cumulative burn area by 2100 projected in CMIP6, and seed arrival probability.** Seed

635 arrival probability includes both short and long distance dispersal and is normalized to the scale

636 of 0-1.

637

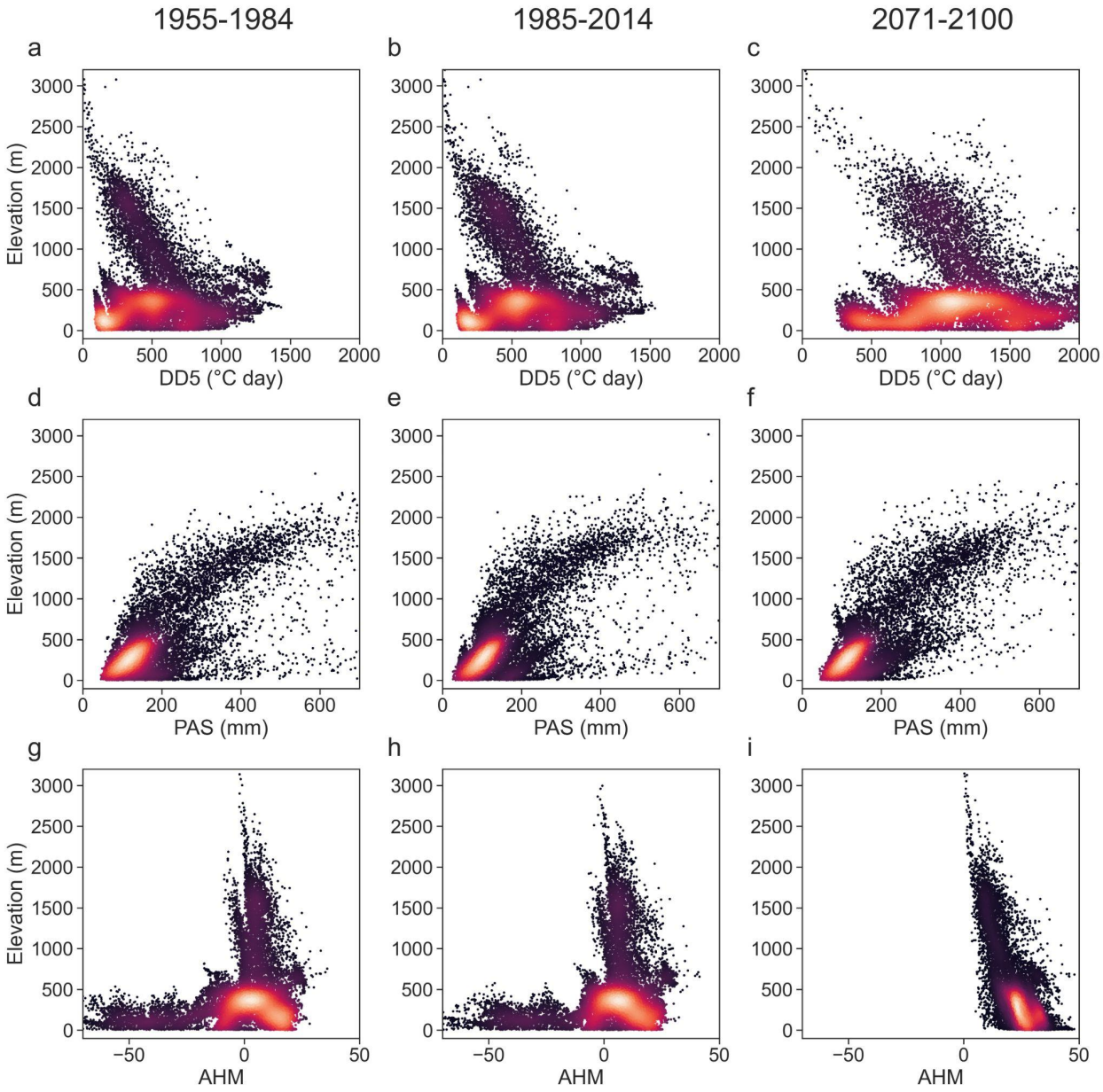

Extended Data Fig. 8 | Historical and projected bioclimatic conditions and elevation across the domain. Joint distribution of (a-c) degree-days above 5°C and elevation, (d-f) annual precipitation as snow and elevation, (g-i) annual heat moisture index and elevation during (a, d, g) 1955-1984, (b, e, h) 1985-2014, and (c, f, i) 2071-2100. Brighter colors represent higher point density.

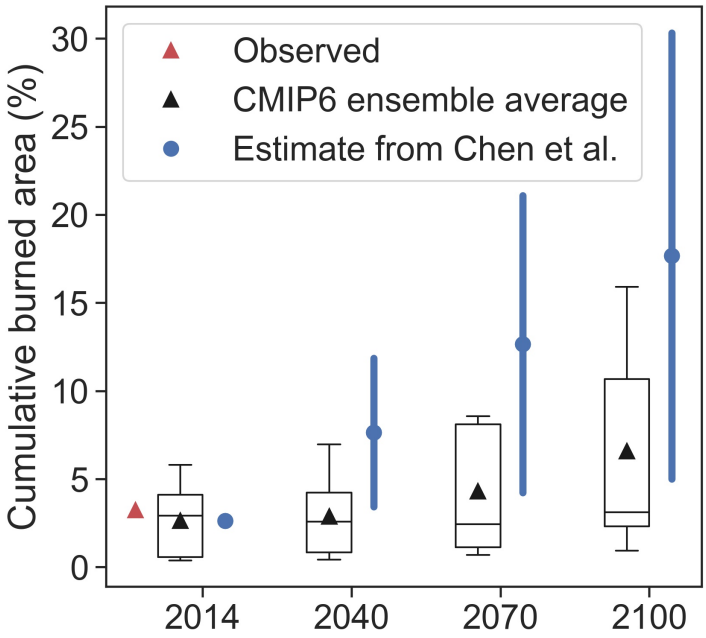

Extended Data Fig. 9 | Domain average of observed and projected 30-year cumulative burn area from 2014 to 2100 based on CMIP6 and Chen et al. (2021). Red triangle shows the domain average of the observed burn area during 1984-2014. Black triangles denote the ensemble average , the upper and lower boundaries of the boxes correspond to the 25th and 75th quantiles, and the whiskers show the range of projections across CMIP6 models. Blue dots and vertical lines represent the predicted mean and uncertainty of burn area in 2100, linearly interpolated from 2014 to 2100, based on Chen et al. (2021) where vegetation-fire feedback was considered.

Supplementary Files

This is a list of supplementary files associated with this preprint. Click to download.

- codeanddemoinputdata.docx